Scattering of a cylinder covered with an arbitrary distribution of admittance and application to the design of a tramway noise abatement system

Alexandre Jolibois, Denis Duhamel, Victor W. Sparrow, Jérôme Defrance, Philippe Jean

ACOUSTICS 2012

Scattering of a cylinder covered with an arbitrary distribution of admittance and application to the design of a tramway noise abatement system

A. Jolibois[a], D. Duhamel[a], V. W. Sparrow[b], J. Defrance[c] and P. Jean[c]

[a]Université Paris-Est - UMR Navier, Ecole des Ponts ParisTech, 6&8 av. Blaise Pascal - Champs-sur-Marne, 77455 Marne La Vallée Cedex 2, France
[b]Graduate Program in Acoustics, The Pennsylvania State University, 201 Applied Science Building, University Park, 16802, USA
[c]CSTB, 24, rue Joseph Fourier, 38400 Saint Martin d'hères, France
alexandre.jolibois@enpc.fr

An urban low-height barrier meant to attenuate tramway noise emission for nearby walking pedestrians or cyclists is studied. A semi-analytical solution for the two-dimensional scattering of a line source by a cylinder covered by an arbitrary distribution of impedance and its image with respect to a vertical baffle is derived. This description is used to model the shadowing due to a semi-cylindrical noise barrier close to a tramway. This solution is used in a gradient-based optimization approach of the admittance distribution to maximize the broadband insertion loss in a given receiver zone. A feasible optimized surface treatment made of a porous layer and a micro-perforated resonant panel is proposed, with an improvement of 14 dB(A) with respect to an entirely rigid barrier. The optimization gain with respect to a uniform absorbent admittance is about 8 dB(A). Extra tests with the boundary element method show that this gain is reduced but still significant if more realistic conditions are considered.

1 Introduction

In the past forty years, there has been a lot of work and effort on trying to understand what affects the efficiency of a noise barrier and how to come up with more efficient designs, especially in the case of highway noise barriers. However, there is more and more concern to reduce noise exposure not only close to highways but also in urban areas. In this case, using walls several meters high is not a feasible option, and therefore the possibility of using a low height protection directly between the source and the receiver started to gain interest [1, 2, 3, 4]. Because the propagation distances are small, near field interference effects are expected to be stronger than in the highway case, and those effects will depend greatly on the shape and the surface admittance (the inverse of the impedance). Optimization of the impedance coverage to maximize the attenuation is therefore likely to be efficient, as shown by Thorsson [4].

As an example application, in this paper we consider a low-height barrier meant to attenuate tramway noise. A recent study [5] showed that most of the noise emitted by a modern tramway comes from the rail track and the *bogie* (undercarriage structure) areas, which are close to the ground and therefore a low height barrier would be likely to attenuate these sources effectively.

Therefore, in this study we consider a low-height (one meter high) semi-cylindrical barrier and we allow the surface admittance to be optimized by a deterministic gradient method. Using the semi-cylindrical geometry has several assets: aesthetically and structurally such a barrier would be integrated more easily in an urban environment, and the sound field can be calculated by semi-analytical methods even in the case of a complex admittance distribution.

2 Description and modeling of the barrier implementation

The atmosphere is assumed homogeneous with a speed of sound of $c_0 = 343$ m/s. The considered physical problem is the calculation of the acoustic pressure field p close to a low-height urban noise barrier in the presence of a tramway (see figure 1). According to Pallas et al. [5], most of the noise emitted by a modern tramway rolling at 40 km/h on rigid paving comes from three sources close to the ground : rail track, powered and un-powered bogie. We model those sources as one infinite, omni-directional line source lying on the ground, with a spectral content given by the incoherent sum of the three identified sources (see figure 2). One can infer that most of the A-weighted acoustic energy is contained in the frequency range 100-5000 Hz, which will be range of interest in the rest of this study. It is also assumed that the geometry is invariant along the axis of the track, which makes the problem purely two dimensional. This assumption has been shown to be correct when predicting excess attenuation in narrow frequency bands, which is what we will use in the calculation of the broadband insertion loss.

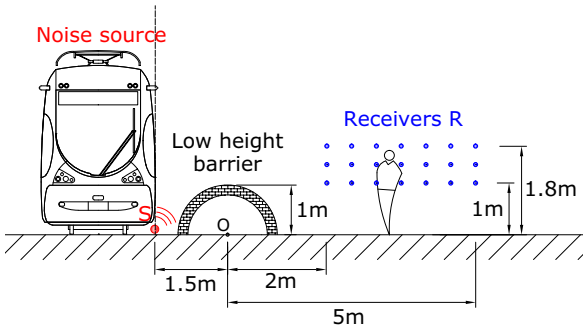

Figure 1: Considered geometrical configuration for the implementation of a tramway low-height noise barrier. The dotted line corresponds to the idealization of the tramway side as a vertical baffle.

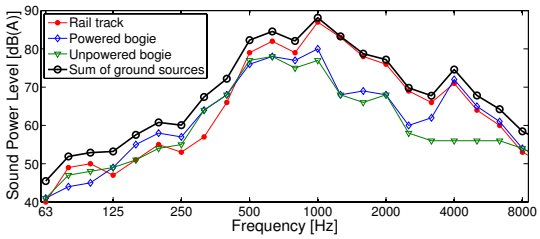

Figure 2: Comparison of third octave spectra of the different sources identified in [5] and their incoherent summation.

The presence of the tramway will cause the sound to bounce on its surface and diffract at the roof edge and at the gap between the carriage and the ground. Calculation of the sound field in such an environment with a realistic cross section of the tramway could be achieved with the boundary element method (BEM). However, in order to reduce the computation time, one can model the tramway as an infinite rigid vertical baffle placed at the location of the vertical portion of the tramway. This idealization is equivalent to introducing an *image* barrier, symmetrical to the original one with respect to the tramway side surface. Finally, the ground is modeled as perfectly rigid as well. This assumption allows application of the image theory once again, transforming both semi-cylindrical barriers into whole cylinders.

The radius of the barrier is $a = 1$ m. The distance between the noise source and the center of the barrier is $d = 1.5$ m, which leaves a gap of 0.5 m between the tramway and the barrier. The receiver locations have been chosen to represent a range of possible locations of pedestrian ears: horizontal distance x from the center of the barrier between 2 m and 5 m , and height y between 1 m and 1.8 m (see figure 1).

2.1 Mathematical representation of the geometry

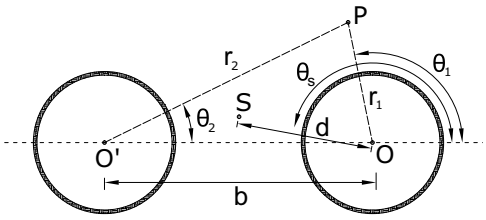

Figure 3: Mathematical representation of the scattering problem and definition of two coordinate systems and notations.

The two considered approximations - rigid ground and tramway side as a vertical baffle - end up making the problem equivalent to the scattering of a line source by two infinite cylinders covered by an arbitrary distribution of admittance. Notations for the geometrical variables are shown in figure 3. This problem is treatable by a semi-analytical approach which we will describe. The solution is derived in the frequency domain, so that the frequency f is fixed and the wavenumber is $k = 2\pi f/c_0$. The time convention is $e^{-i\omega t}$. The surface of the original cylinder is assumed to be locally reacting described by a normalized admittance function $\beta(\theta_1)$ with $\theta_1 \in [0, 2\pi]$. The finite admittance boundary condition at the surface can be written as:

$$(\forall \theta_1 \in [0,2\pi]) \quad \frac{\partial p}{\partial r_1}(a,\theta_1) + ik\beta(\theta_1)\, p(a,\theta_1) = 0 \qquad (1)$$

Because of the implicit angular periodicity and the symmetry, the distribution can be decomposed as an angular Fourier series:

$$\beta(\theta_1) = \sum_{p=0}^{\infty} \beta_p \cos(p\theta_1) \qquad (2)$$

Only cosine terms are considered because β has to be symmetric about $\theta_1 = 0$. The coefficients β_p will be referred to as the *admittance coefficients* and will uniquely define an admittance distribution. Those coefficients also depend on frequency. The distribution on the image cylinder $\tilde{\beta}(\theta_2)$ can be decomposed in a similar fashion, but because of the symmetry with respect to the vertical baffle, coefficients must be replaced by $(-1)^p \beta_p$.

3 Solution of the acoustic scattering by two non uniform impedant cylinders

The pressure field is broken up like $p = p^{\text{in}} + p_1^{\text{sc}} + p_2^{\text{sc}}$ where p^{in} is the incident field, p_1^{sc} is the field scattered by the true cylinder and p_2^{sc} is the field scattered by the image cylinder. We will assume for now a unit amplitude for the source. The incident field is:

$$p^{\text{in}} = \frac{i}{4}\left[H_0(k\,\text{SR}) + H_0(k\,\text{S'R})\right] \qquad (3)$$

where S' is the image source with respect to the ground, SR and S'R the distances between the receiver and the actual and image source respectively and H_0 is the Hankel function of the first kind of order zero. Since both scattered fields are purely outgoing and the problem is symmetrical about $\theta = 0$, they can be assumed to be a series of the form:

$$p_l^{\text{sc}}(r_l,\theta_l) = \sum_{n=0}^{\infty} \frac{\alpha_n^l}{\epsilon_n} \frac{H_n(kr_l)}{H_n(ka)} \cos(n\theta_l) \qquad (4)$$

with $l = 1, 2$, $\epsilon_n = (2, 1, 1, 1...)$ and H_n is the Hankel functions of the first kind of order n. Determination of the coefficients α_n^l comes from the boundary conditions on the original and image cylinders. This requires to express the incident field and one of the two scattered fields in the same basis of functions than the other scattered field. This can be achieved using Graf's addition theorem (see [6] p.363). Applying the finite impedance boundary condition on both cylinders and identifying Fourier coefficients for the two angular variables yields the following infinite matrix equation satisfied by the coefficients α_n^1 and α_n^2:

$$\begin{bmatrix} \mathbf{M}^{11} & \mathbf{M}^{12} \\ \mathbf{M}^{21} & \mathbf{M}^{22} \end{bmatrix} \begin{bmatrix} \boldsymbol{\alpha}^1 \\ \boldsymbol{\alpha}^2 \end{bmatrix} = \begin{bmatrix} \mathbf{e}^1 \\ \mathbf{e}^2 \end{bmatrix} \qquad (5)$$

$\boldsymbol{\alpha}^1$ and $\boldsymbol{\alpha}^2$ are two vectors containing the coefficients α_n^1 and α_n^2 respectively; $\mathbf{e}^1$ and $\mathbf{e}^2$ are the two vectors containing the coefficients e_p^1 and e_p^2 corresponding to the influence of the incident field on each cylinder. Detailed calculations of the different coefficients of system (5) are provided elsewhere [7].

In order to solve equation (5) numerically, several truncations must be made on the different series representing the admittance distribution β, the incident field p^{in} and the two scattered fields p_l^{sc}. First, we define $N_{\max}$ the maximum order of the admittance Fourier series (2), which is considered a given parameter. Then, we need to ensure that the incident and scattered fields decompositions are accurate at the surface of each cylinder, which can be done by conducting simple convergence studies.

4 Objective function

The semi-analytical solution provides a way to calculate the complex pressure amplitude $p(R, f)$ at each frequency and at each receiver point, for a unit source amplitude. One can then define an average attenuation:

$$A_n = \frac{\sum_i |p(R_i, f_n)|^2}{\sum_i |p^{\text{in}}(R_i, f_n)|^2} \qquad (6)$$

Then, we consider a broadband attenuation based on the sound power levels $L_{w,n}$ measured by Pallas et al. [5] and shown in figure 2. Defining an amplitude-like quantity $S_n = 10^{L_{w,n}/10}$, the broadband attenuation is given by:

$$g = \frac{\sum_n S_n A_n}{\sum_n S_n} \qquad (7)$$

which is equivalent to the objective function considered by Baulac et al. [1, 2]. In the optimization process, the attenuation is calculated at each sixth-octave frequency between 100 and 5000 Hz. We would like to minimize the function g, which only depends on the admittance distribution and therefore on the coefficients β_p defined in 2.1. One can also calculate from the objective function a broadband insertion loss in dB(A) defined by $\text{IL} = -10 \log g$.

4.1 Gradient of the attenuation

A deterministic gradient-based optimization approach has been chosen. Indeed, in such a semi-analytical context, sensitivities of the objective function with respect to changes in parameters (gradient components) can be computed quickly and accurately which would make the optimization search relatively fast as well. The objective function is directly related to the attenuations A_n at a given frequency, therefore we only need to calculate its gradient with respect to the admittance coefficients $\partial A_n/\partial\beta_j$. Since the incident field does not depend on the barrier, we have for any index $j \in [0, N_{\max}]$:

$$\frac{\partial A_n}{\partial \beta_j} = \frac{2}{\sum_i |p^{\text{in}}(R_i, f_n)|^2} \sum_i \text{Re}\left[p(R_i, f_n)^* \sum_{l=1,2} \frac{\partial p_l^{\text{sc}}(R_i, f_n)}{\partial \beta_j} \right] \tag{8}$$

where * is the complex conjugation. We are left with the calculation of the gradient of the scattered fields with respect to the admittance coefficients. Using the definition (4), we have:

$$\frac{\partial p_l^{\text{sc}}}{\partial \beta_j}(r_l, \theta_l) = \sum_{n=0}^{\infty} \frac{1}{\epsilon_n} \frac{\partial \alpha_n^l}{\partial \beta_j} \frac{H_n(kr_l)}{H_n(ka)} \cos(n\theta_l) \tag{9}$$

with $l = 1, 2$. The calculation of the gradient of the attenuation is therefore based on the gradient of the vector-valued function $\boldsymbol{\alpha}(\boldsymbol{\beta})$. Taking the derivative of equation (5) with respect to β_j yields:

$$\mathbf{M} \frac{\partial \boldsymbol{\alpha}}{\partial \beta_j} = \frac{\partial \mathbf{e}}{\partial \beta_j} - \frac{\partial \mathbf{M}}{\partial \beta_j} \boldsymbol{\alpha} \tag{10}$$

Equation (10) is another system of the form $\mathbf{M}\,\mathbf{x} = \mathbf{b}$, which can be solved numerically to obtain the partial derivatives $\partial\boldsymbol{\alpha}/\partial\beta_j$.

5 Application: finite number of panels with realistic impedance models

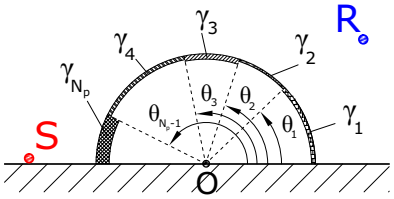

Figure 4: Cylindrical barrier covered with a finite number of panels N_p.

As an example of application, the barrier is assumed to be covered by a finite number of panels (see figure 4). Each of those panels (indexed by $p \in [1 : N_p]$) lies between the two angles θ_{p-1} and θ_p (with the convention $\theta_0 = 0$ and $\theta_{N_p} = \pi$). The angles θ_1 to θ_{N_p-1} are design variables subject to the constraint $0 = \theta_0 \leqslant \theta_1 \leqslant \theta_2 \leqslant ... \leqslant \theta_{N_p} = \pi$.

Besides, each panel has an admittance described by a physical model, which typically depends on a small number of parameters. Following the concept of coupling dissipative and reactive impedance to broaden the frequency range of sound attenuation introduced by Namba and Fukushige [8] and further developed by Selamet et al. [9], we will consider two types of panels usually used in noise control: *micro-perforated panels* (MPP) and *absorbent layers*. A MPP typically absorbs sound in selected frequency bands, which can be more or less broad depending on the hole radius [10]. An absorbent layer is simply a layer of porous material, typically described by the Delany & Bazley model [17]. Such material provides some reasonable broadband absorption over the whole frequency range of interest. The layer version of this model has been shown to model many natural surfaces such as soils or grass relatively accurately [11].

5.1 Admittance models

5.1.1 Micro-perforated panel

The impedance of a MPP can be written in terms of four parameters: the porosity s, the hole radius a_0, the thickness of the panel l_0 and the cavity depth D. Assuming that the panel itself is rigid and one can use Sibian's model for the end correction, the normalized impedance can then be written in the $e^{-i\omega t}$ convention as [12, 13, 14]:

$$z_{\text{MPP}}(f) = -i\,\frac{kl_0}{s}\left(\frac{1}{\Theta(x')} + \frac{16}{3\pi}\frac{a_0}{l_0}\frac{\Psi(\xi)}{\Theta(x)}\right) + i\,\text{cotan}\,(kD) \tag{11}$$

$$\text{with} \quad \Theta(w) = 1 - \frac{2}{w\sqrt{i}}\frac{J_1(w\sqrt{i})}{J_0(w\sqrt{i})}$$

$k = 2\pi f/c_0$ is the wavenumber, $\xi = \sqrt{s}$, $x/a_0 = \sqrt{2\pi f\rho_0/\mu}$ and $x'/a_0 = \sqrt{2\pi f\rho_0/\mu'}$ are the so-called perforate constants, $\mu' \approx 2.2\,\mu$ is an equivalent viscosity corresponding to thermal effects. Finally, the Fok's function [15, 16] $\Psi(\xi)$ is a correction to take into account interaction effects between the different holes. The normalized admittance is then simply $\gamma_{\text{MPP}}(f) = 1/z_{\text{MPP}}(f)$.

5.1.2 Rigid-backed Delany and Bazley model

Here we consider a layer of porous material of depth d ended by a rigid backing. Following Delany and Bazley [17], the normalized impedance and complex wavenumber only depend on one parameter σ and are given by:

$$\begin{cases} \tilde{z}(f) = 1 + 0.0511\left(\dfrac{\sigma}{f}\right)^{0.75} + i\,0.0768\left(\dfrac{\sigma}{f}\right)^{0.73} \\ \dfrac{\tilde{k}}{k_0} = 1 + 0.0858\left(\dfrac{\sigma}{f}\right)^{0.7} + i\,0.175\left(\dfrac{\sigma}{f}\right)^{0.59} \end{cases} \tag{12}$$

with $k_0 = 2\pi f/c_0$ is the wavenumber in air. However, because of the finite depth d of the layer, and by assuming that the backing is infinitely rigid, the admittance is:

$$\gamma_{\text{DB}}(f) = \frac{1}{\tilde{z}(f)\,\coth(-i\tilde{k}d)} \tag{13}$$

5.2 Description of the optimization problem

Four panels are here considered and they are located as follows: panels # 1 and # 3 are MPPs, and panels #2 and #4 are absorbent layers. The design variables are here the different parameters involved in the admittance function of each panel as well as the three angular variables θ_1, θ_2 and θ_3 (see figure 4). For a given vector set of parameters and angles, there is a unique set of four panel admittances $(\gamma_1, \gamma_2, \gamma_3, \gamma_4)$ at each frequency and therefore a unique set of admittance coefficients β_p which can be determined by a straightforward Fourier series coefficients calculations. We arbitrarily chose the parameter $N_{\max} = 10\,N_p$. Besides, the derivative of A_n

with respect to a parameter x can be related to the derivative of the α_n^l by relations similar to equations (8) and (9) replacing β_j with x. Then, using the chain rule one can write:

$$\frac{\partial \alpha_n^l}{\partial x} = \sum_{j=0}^{N_{\max}} \frac{\partial \alpha_n^l}{\partial \beta_j} \frac{\partial \beta_j}{\partial x} \tag{14}$$

so that the derivatives $\partial \alpha_n^l / \partial \beta_j$, which can be calculated as explained in section 4.1, can be used again in this case. One simply needs to find $\partial \beta_j / \partial x$ for example by derivation of the admittance models (11) and (13). The optimization algorithm is the interior-point algorithm. Furthermore, to allow a better search of the design space, five random starting points are used.

To completely define the optimization problem, we still need to choose a range for the admittance parameters, which depends on the type of parameter:

- Porosity: $s_{\min} = 0.01$; $s_{\max} = 0.4$
- Hole radius [mm]: $a_{0,\min} = 0.5$; $a_{0,\max} = 5$
- Panel thickness [cm]: $l_{0,\min} = 0.2$; $l_{0,\max} = 1$
- Cavity depth [cm]: $D_{\min} = 1$; $D_{\max} = 10$
- Flow resistivity [kPa.s/m^2]: $\sigma_{\min} = 50$; $\sigma_{\max} = 200$
- Porous layer depth [cm]: $d_{\min} = 1$; $d_{\max} = 10$

The choice of those ranges is based on physically feasible values. Especially, the range of flow resistivities has been chosen according to grassland-type soils values determined by Attenborough et al. [11].

5.3 Results

Each run of the optimization algorithm converged within a few hundred iterations. The best obtained solution parameters are shown in table 1. If one assumes that the semi-cylinder is covered only with a porous layer of smallest resistivity $\sigma = \sigma_{\min}$ the efficiency obtained is 15.3 dB(A), which is lower than the obtained solution. Therefore, there seems to be a definite benefit in coupling porous layers and resonant panels, which is again of the order of 8 dB(A). Besides, substituting panels 1 and 2 by rigid panels in the obtained solution induces a slight decrease of 0.1 dB(A) in the broadband attenuation, which suggests that the admittance on the receiver side (far from the source) does not influence the attenuation significantly.

Also, comparison of the solution third-octave insertion losses with reference cases (rigid or porous) shows that the improvement of the barrier covered by the four optimized panels is mostly located in the mid-frequency range 300-1500 Hz where most of the frequency content of the source is located (see figure 5).

5.4 Validity of the rigid ground and vertical baffle approximations

The semi-analytical scattering solution which has been used in the optimization was derived under two important assumptions: rigid ground and modeling of the tramway as a vertical infinite baffle. We therefore end this section by comparing the predicted performance of the barrier covered with the optimized distribution exposed in 5.3 to more realistic situations. To do so, four cases detailed in figure 6 are considered. In each case, the attenuation at each frequency is the ratio $|p_{\text{ref}}/p|$ in dB, with p is the field at the receiver with the barrier present and p_{ref} is the field without the barrier. The 2D BEM software MICADO developed by Jean [18] has been used for the calculations. Third-octave insertion losses results are shown figure 7. The absorbent treatment on the ground is modeled with a Delany & Bazley layer with $\sigma = 50\,\text{kPa.s/m}^2$ and $d = 5\,\text{cm}$, which corresponds to the most absorbent porous material allowed in the optimization. To simplify the calculation, one receiver point only of cartesian coordinates (3 m, 1.8 m) is considered here. Calculation of the broadband efficiency based on the tramway spectrum in each case yields : a) 20.9 dB(A) - b) 19.4 dB(A) - c) 17.3 dB(A) - d) 11.9 dB(A).

Comparing cases a) and b) from figure in 7, one can conclude that the infinite baffle approximation for the tramway in presence of a rigid ground is relatively accurate, even though it induces a slight over-prediction of 1.5 dB(A) in the broadband efficiency. Comparison between b) and c) shows that the benefit due to the barrier only is reduced when the ground is treated. This effect is consistent over the considered frequency range, above 200 Hz, inducing a decrease of the benefit of the barrier of 2.1 dB(A). However, comparing c) and d), one can notice that the optimized non uniform admittance distribution we obtained still performs better than a barrier covered with a uniform absorbing treatment in the mid-frequency range 300-1500 Hz, as shown in figure 7, inducing a net benefit of more than 5 dB(A) on the broadband efficiency, even in the case of a treated ground.

Table 1: Model parameters and angular widths of the best obtained solution

Panel	Parameter	
# 1 (MPP)	Porosity s	0.26
	Hole radius a_0 [mm]	4.48
	Panel thickness l_0 [cm]	0.41
	Cavity depth D [cm]	8.34
	Angular width [$\times \pi$ rad]	0.16
# 2 (porous)	Flow resistivity σ [kPa.s/m^2]	120.0
	Layer thickness d [cm]	5.34
	Angular width [$\times \pi$ rad]	0.06
# 3 (MPP)	Porosity s	0.12
	Hole radius a_0 [mm]	0.54
	Panel thickness l_0 [cm]	0.70
	Cavity depth D [cm]	9.38
	Angular width [$\times \pi$ rad]	0.54
# 4 (porous)	Flow resistivity σ [kPa.s/m^2]	51.9
	Layer thickness d [cm]	6.04
	Angular width [$\times \pi$ rad]	0.23
Broadband IL [dB(A)]		23.1

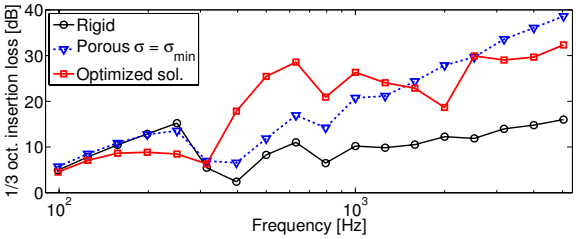

Figure 5: Third-octave insertion loss in dB of the optimized solution and comparison with reference cases: rigid $\beta = 0$ (thin solid line), IL = 8.7 dB(A) - uniform porous layer $\sigma = \sigma_{\min}$ (dotted line), IL = 15.3 dB(A) - optimized solution (thick solid line), IL = 23.1 dB(A).

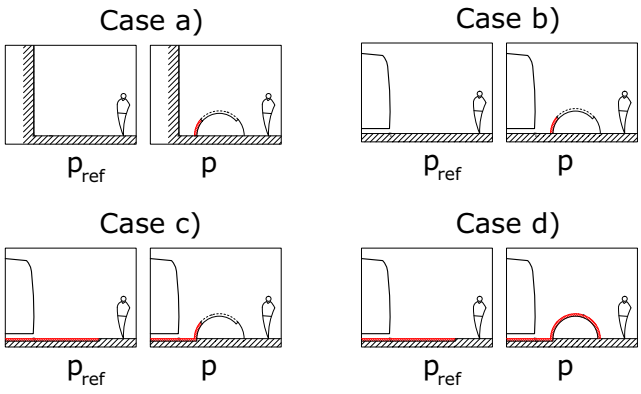

Figure 6: Description of the four cases used to assess the validity of the rigid ground and vertical baffle approximations. Surface admittance coding: black line = rigid ; red hatched area = absorbent ; dotted black line = MPP. a) Rigid ground, infinite baffle and optimized barrier treatment - b) rigid ground, realistic tramway and optimized barrier treatment - c) absorbing ground, realistic tramway and optimized barrier treatment - d) absorbing ground, realistic tramway and uniform absorbing barrier treatment.

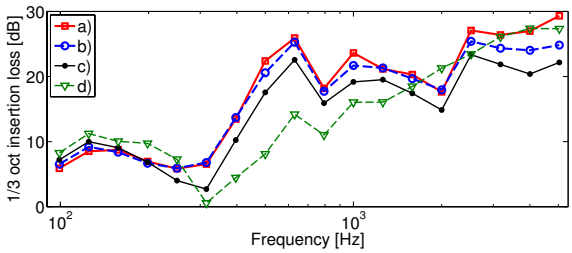

Figure 7: Third octave insertion losses in dB calculated in the four cases detailed in figure 6.

6 Conclusion

A semi-analytical solution has been developed in order to calculate the sound attenuation due to a semi-cylindrical noise barrier covered by any distribution of admittance in the presence of a vertical baffle and a rigid ground. Such a mathematical representation is used to model the sound field close to a tramway, in presence of a semi-cylindrical low height barrier between the source and the receivers. The fast evaluation of the efficiency as well as its gradient with respect to the admittance distribution therefore allows the optimization of the admittance distribution on the surface of the barrier.

As an example application, the barrier is assumed to be covered by a set of MPPs and porous layers, and the optimization is used to determine the parameters describing the admittance of each panel. It is found that strongly absorbent materials with low flow resistivities seem indeed necessary, however using a uniform purely absorbent layer with a low flow resistivity is not the optimal solution. Coupling this absorbing layer with a tuned resonant panel can significantly improve the attenuation while only slightly degrading the performance at higher frequencies. Also, it seems that the attenuation is somewhat insensitive to the barrier admittance on the opposite side of the source.

Additional calculations using the BEM with more realistic conditions showed that the predicted benefit of the optimized barrier is lowered by a few dB(A) if a more realistic tramway cross section and an absorbent ground are considered, but remains significant (more than 16 dB(A)).

Efficiencies obtained in this study are probably higher than what would be observed in practice due to the simplified description of the geometry and source. However, the development of the semi-analytical model that follows from those assumptions provides an efficient way to automatically choose treatment surface design parameters in order to improve the performance of the low height barrier.

References

[1] M. Baulac, J. Defrance, P. Jean, "Optimization of low height noise protections in urban areas", In *Forum Acousticum 2005, Budapest*, 1075-1080.

[2] M. Baulac, J. Defrance, P. Jean, F. Minard, "Efficiency of noise protections areas: prediction and scale model measurements", *Acta Acust. United Ac.* **92**, 530-539 (2006)

[3] P. J. Thorsson, "Optimisation of low-height noise barriers using the equivalent sources method", *Acta Acust.* **86**, 811-820 (2000)

[4] P. J. Thorsson, "Combined effects of admittance optimisation on both barrier and ground", *Appl. Acoust.* **64**, 693-711 (2003)

[5] M. A. Pallas, J. Lelong, R. Chatagnon, "Characterization of tram noise emission and contribution of the noise sources", *Appl. Acoust.* **72**, 437-450 (2011)

[6] M. Abramovitz, I. A. Stegun, *Handbook of mathematical functions*, National Bureau of Standards, Applied Mathematics (1964)

[7] A. Jolibois, D. Duhamel, V. W. Sparrow, J. Defrance, P. Jean, "Scattering by a cylinder covered with an arbitrary distribution of impedance and application to the optimization of a tramway noise abatement system", *J. Sound. Vib.* (submitted)

[8] M. Namba, K. Fukushige, "Application of the equivalent source method to the acoustics of duct systems with non-uniform wall impedance", *J. Sound Vib.* **73**(1), 125-146 (1980)

[9] A. Selamet, I. J. Lee, N. T. Huff, "Acoustic attenuation of hybrid silencers", *J. Sound Vib.* **262**(3), 509-527 (2003)

[10] D.-Y. Maa, "Potential of microperforated panel absorber", *J. Acoust. Soc. Am.* **104**(5), 2861-2866 (1998)

[11] K. Attenborough, I. Bashir, S. Taherzadeh, "Outdoor ground impedance models", *J. Acoust. Soc. Am.* **129**(5), 2806-2819 (2011)

[12] T. H. Melling, "The acoustic impedance of perforates at medium and high sound pressure levels", *J. Sound Vib.* **29**(1), 1-65 (1975)

[13] F. Asdrubali, G. Pispola, "Properties of transparent sound-absorbing panels for use in noise barriers", *J. Acoust. Soc. Am.* **121**(1), 214-221 (2007)

[14] A. F. Sobolev, "A semi-empirical theory of a one-layer cellular sound-absorbing lining with a perforated face panel", *Akust. Zh.* **53**(6), 762-771 (2007)

[15] V. A. Fok, "Teoreticheskoe issledovanie provodimosti kruglogo otverstiya v peregorodke, postavlennoi poperek truby (theoretical study of the conductance of a circular hole in a partition across a tube)", *Dokl. Akad. Nauk SSSR* **31**(9), 875-882 (1941)

[16] S. N. Rzhevkin, *A course of lectures on the theory of sound*, Pergamon Press, London (1963)

[17] M. E. Delany, E. N. Bazley, "Acoustical properties of fibrous absorbent materials", *Appl. Acoust.* **3**, 105-116 (1970)

[18] P. Jean, "A variational approach for the study of outdoor sound propagation and application to railway noise", *J. Sound Vib.* **212**(2), 275-294 (1998)